The issue of cavitation number value in studies of water treatment by hydrodynamic cavitation

Article *in* Ultrasonics Sonochemistry · May 2016

DOI: 10.1016/j.ultsonch.2016.05.020

4 authors:

Andrej Šarc

University of Ljubljana

Tadej Stepisnik Perdih

University of Ljubljana

Martin Petkovšek

University of Ljubljana

Matevz Dular

University of Ljubljana

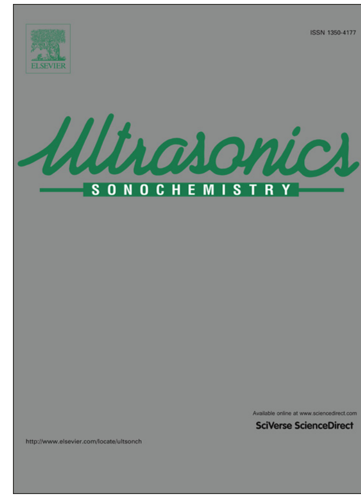

The issue of cavitation number value in studies of water treatment by hydrodynamic cavitation

Andrej Šarc, Tadej Stepišnik-Perdih, Martin Petkovšek, Matevž Dular

PII: S1350-4177(16)30162-6
DOI: http://dx.doi.org/10.1016/j.ultsonch.2016.05.020
Reference: ULTSON 3230

To appear in: *Ultrasonics Sonochemistry*

Received Date: 25 February 2016
Revised Date: 29 April 2016
Accepted Date: 12 May 2016

The issue of cavitation number value in studies of water treatment by hydrodynamic cavitation

Andrej Šarc, Tadej Stepišnik-Perdih, Martin Petkovšek, Matevž Dular*

University of Ljubljana
Askerceva 6, 1000 Ljubljana, Slovenia
Voice: +386 (1) 4771 314
E-mail: matevz.dular@fs.uni-lj.si
Web: www2.arnes.si/~mdula

Abstract
Within the last years there has been a substantial increase in reports of utilization of hydrodynamic cavitation in various applications. It has came to our attention that many times the results are poorly repeatable with the main reason being that the researchers put significant emphasis on the value of the cavitation number when describing the conditions at which their device operates.
In the present paper we firstly point to the fact that the cavitation number cannot be used as a single parameter that gives the cavitation condition and that large inconsistencies in the reports exist. Then we show experiments where the influences of the geometry, the flow velocity, the medium temperature and quality on the size, dynamics and aggressiveness of cavitation were assessed. Finally we show that there are significant inconsistencies in the definition of the cavitation number itself.
In conclusions we propose a number of parameters, which should accompany any report on the utilization of hydrodynamic cavitation, to make it repeatable and to enable faster progress of science and technology development.

Key words: cavitation; cavitation number, inconsistency, utilization of cavitation

1 Introduction

The use of acoustic cavitation for water and wastewater treatment is a well known procedure [1]. Yet, the use of hydrodynamic cavitation as a sole technique or in combination with other techniques such as ultrasound has only recently been suggested and employed. As the field of utilization of hydrodynamic cavitation is growing, it came to our (we are mechanical engineers who deal primarily with fluid dynamics problems) attention that researchers put significant emphasis on the value of the cavitation number (also known as cavitation parameter, σ value or Thoma number – Th) when describing their techniques, devices and procedures for water treatment.

Already a brief literature survey reveals the following examples. Saharan et al. [2] report on an optimal cavitation number of 0.13–0.18 at which decolorisation rate is maximum. Raut-Jadhav et al. [3] recommend (besides other conditions) a value of $\sigma = 0.067$. Sivakumar & Pandit [4] conclude that lower values of cavitation number mean higher extent of degradation of pharmaceuticals. Badve et al. [5] report maximal reduction in COD at $\sigma = 0.4$. Bagal & Gogate [6] claim that the greatest benefits of cavitation are obtained at $\sigma = 0.1$ to 1. Gogate [7] writes that cavitation generally appears at $\sigma = 1$ and that significant cavitational effects appear at σ values of less than 1. Capocelli et al. [8] found an optimal and cavitation number of 0.25 in terms of removal rate and energy efficiency. Wang & Zang [9] report on the dependency of degradation rate of alachlor on the value of cavitation number. Gore et al. [10] write that the degradation of reactive orange 4 depends on cavitation number and other parameters. Senthil Kumar et al. [11] show the influence of cavitation number on chemical effects. Sawant et al. [12] state that cavitation number predicts the relative intensity of cavitation taking place in various cavitation devices and can be used as preliminary tool to compare the relative performance of a cavitational system. Wu et al. [13] compare cavitation numbers for different geometries and claim that for effects to occur σ values should much smaller than 1. Cavitation number of 0.14 was used for bacterial inactivation by Filho et al. [14]. And finally Aroyo et al. [15] and Mezule et al. [16], show almost no details on the operating conditions of their devices.

In this paper we would like to point out the issues of the definition of the cavitation number and call out to all the research community to properly describe their experiments, which are, due to the lack of data on the operating conditions poorly repeatable or even unrepeatable at all. In other words: describing the cavitation conditions solely by the value of the cavitation number is inappropriate and misleading.

2 Cavitation number

In the simplest reasoning one can assume that vapor bubbles appear as the pressure in the liquid drops below the vapor pressure of the liquid at the given temperature. This condition can be formulated as:

$$p_{\min} = p_v, \qquad (1)$$

where p_{min} is the minimum static pressure (in time or space reference) and p_v is the vapor pressure at a given temperature of the liquid. Many times researchers tend to use non-dimensionalised values – in the present case this is the pressure coefficient C_p (also known as the Euler number) defined as:

$$c_p(\vec{r},t) = \frac{p(\vec{r},t) - p_0}{\frac{\rho v^2}{2}}, \qquad (2)$$

where p_0 and v_0 are reference pressure and velocity (again at a reference time and space). Combining Eqns. 1 and 2 reveals the pressure coefficient for the moment when cavitation first occurs:

$$c_{p,\min} = \frac{p_{\min} - p_0}{\frac{\rho v^2}{2}}. \qquad (3)$$

$c_{p,\ min}$ is a negative number, which is a function of geometry and the velocity. If one could obtain the value of $c_{p,\ min}$ then the reference pressure $p_{0,cav}$ at which cavitation would first appear could be determined:

$$p_{o,cav} = p_v + \frac{1}{2}\rho v^2\left(-c_{p,\min}\right), \qquad (4)$$

which is now dependent on the geometry, fluid, fluid temperature and the velocity of the flow.

What Diether Thoma derived in 1920' is a form of the Euler number (Eqn. 2). The most fundamental non-dimensional parameter, which is since then utilized for evaluating the potential for cavitation – the cavitation number σ is written as:

$$\sigma = \frac{p_0 - p_v}{\frac{\rho v^2}{2}}. \tag{5}$$

Every flow, cavitating or not, can be attributed by a cavitation number, its value again depends on the geometry, fluid, fluid temperature and the velocity of the flow. The conditions at which cavitation first appears can also be written as:

$$\sigma_i = -c_{p,\min} \tag{6}$$

where index i stands for "incipient" and σ_i for incipient cavitation number. Lowering the value of cavitation number results in the appearance of cavitation or the increase of extent of already present cavitation.

Cavitation number was primarily applied to open flow problems, such as hydrofoils. Later it was also used for orifices or Venturies where (partial) choking of the flow can occur – form this point on its usefulness can become an issue.

3 Experiment

Tests were performed in a cavitation tunnel at the Laboratory for Water and Turbine Machines, University of Ljubljana.

The experiments (and results) can be divided into 5 general parts:

- <u>Investigation of the geometry influence.</u> Here we make measurements at a constant pressure, constant flow velocity, constant temperature and consequently constant cavitation number, but we slightly change the geometry of the Venturi section.
- <u>Investigation of the influence of flow velocity.</u> Here we make measurements at a constant cavitation number, constant temperature and the same geometry, but we vary the flow velocity and consequently the pressure (we vary the later in order to achieve the same cavitation number).
- <u>Investigation of the influence of fluid temperature.</u> Here we make measurements at a constant cavitation number, constant flow velocity and the same geometry, but we vary the fluid temperature and consequently the pressure (we vary the later in order to achieve the same cavitation number).
- <u>Investigation of the influence of fluid quality.</u> Here we make measurements at a constant cavitation number, constant flow velocity, constant temperature and the same geometry, but we vary the gas content (cavitation nuclei population) of water.
- <u>Investigation of the influence of the cavitation number definition.</u> Here we make measurements at a constant pressure, constant flow velocity, constant temperature and the same geometry. Later we calculate the cavitation number σ, based on different definitions found in literature.

3.1 Test-rig

The cavitation tunnel (Fig. 1) has a closed circuit and the following important features:

- compressor and a vacuum pump, which enable the variation of the system pressure,
- a frequency controlled pump operation by which we can set a desired flow rate,
- heating and cooling systems for the fluid by which the operating temperature can be set.

The listed features enable setting of all influential parameters in the cavitation number definition (Eqn. 5).

A 4.5 kW pump (1) enables the variation of the rotation frequency in order to set the flow rate. Downstream of the pump, a partially filled tank (2) is installed for water heating and for damping the periodical flow rate and pressure fluctuations. Cavitation and its effects are observed in a test section (3). The tank further downstream (4) is used for cooling of the circulation water - a secondary cooling water loop is installed in it. The valves (5) and (6) enable easy and fast disconnection of the test section from the main loop. The flow rate is measured by an electromagnetic flow meter (7) ABB ProcessMaster 300 (DN 40) with a 0.4% uncertainty on measurements. Fluid temperature is obtained with a type Pt100 (8) with an ±0.15% uncertainty. The pressure in the test rig is adjusted in the partially filled tank (2) connected to a compressor (10) and a vacuum pump (11).
The pressure is measured at 5 different positions – 9a (in the tank (2)), 9b,c,d,e (shown in more detail in Fig. 2) by ABB 266AST pressure transducers. The uncertainty of the measurements ±0.04%.

The quality of water can significantly influence the aggressiveness of cavitation – lower gas content results in more aggressive cavitation [17]. In order to assure repeatable measurements the quantity of the dissolved gases was measured by the Van-Slyke method [18] according to [19, 20] the increase of the dissolved gases is proportional to the increase of the cavitation nuclei content.

3.2 Test-section

Four Venturi-type sections were used in the present study (Fig. 2). They all have a constant width of 10mm and the cross-section at the throat is 10×10mm^2 for all of them. Three have the same general geometry with a convergent angles of 18° and divergent angles of 4°, 8°, and 12°, respectively. An additional Venturi section has again a convergent angle of 18° and divergent angles of 8° but the transition at the throat is not continuous (8° S). The Venturi shapes and the side walls were manufactured out of transparent acrylic glass in order to enable visual observation of cavitation.

As already mentioned the static pressure is measured by ABB 266AST pressure transducers at 5 different positions (Fig. 2) – SP_a (in the tank, shown in Fig. 1), SP_b (before the transition into the test-section, 70mm upstream of the throat), SP_c (inside the test- section, 40mm upstream of the throat), SP_d (inside the test-section, 155mm downstream of the throat), SP_e (after the transition from the test- section, 220mm downstream of the throat).
Also noted in Fig. 2 is the position (DP) of the hydrophone installation for the measurements of pressure oscillations (inside the test-section, 130 mm downstream of the throat).

3.3 Evaluation of cavitation conditions

Cavitation conditions were evaluated according to the extent (mean length) of the cavitation region, its dynamics (the cavitation cloud shedding frequency) and the magnitude and frequency of pressure pulsations.

3.3.1 High speed visualization

High speed camera Fastec Imaging HiSpec4 2G mono was used for image acquisition. It can capture images at 523 frames per second (fps) at 3Mpixel resolution and up to 300000 fps at a reduced resolution. For the present experiment the camera recorded at 6000 fps at a reduced resolution of 946×248 pixels.
From the captured sequences of cavitating flow we could determine the mean cavity length and the frequency at which the cavitation pocket oscillates or sheds of clouds (by means of fast Fourier transform of the sequences).

3.3.2 Measurements of pressure oscillations

Pressure was measured by a hydrophone ResonTC4013 with usable frequency range 1 Hz to 170 kHz and receiving sensitivity of -211 dB ± 1 dB re 1V/μPa (using the calibration curve). The signal

from the hydrophone was recorded in terms of voltage. The measured signal was calibrated according to the amplification and to the nominal sensitivity of the hydrophone to give the results in terms of pressure (Pa). The uncertainty of pressure measurements was estimated to ±3% of the measured value.
From the acquired signal we could determine the amplitude and the frequency (by means of fast Fourier transform of the signal) of pressure oscillations which occur due to cavitation bubble (cloud) collapses.

4 Results
The test parameters included numerous conditions where the flow rate, pressure, temperature and water gas content was varied. We varied the pressure in the reservoir (p_a) in the range between 1 and 5 bar, the flow rate between 80 and 150 l/min, temperature of the water from 20 to 70°C and the gas content from 11.1 mg_{gas}/L_{water} (degassed) to 30.1 mg_{gas}/L_{wate} (untreated water).

For easier representation of the results we will, for the time being, define the cavitation number σ by the pressure inside the section upstream of the Venturi (p_c, measured in point SP_c, Fig. 2), the velocity at the throat of the Venturi (v_{th}, given by the flow rate divided by the throat cross-section) and the vapor pressure and density at the fluid temperature:

$$\sigma = \frac{p_c - p_v}{\frac{\rho v_{th}^2}{2}} \quad (7)$$

According to Eqn. 7 the cavitation number was varied between σ=1.5 and σ=1.7.

4.1 Investigation of the geometry influence
The first fact, which is many times overlooked by researches, is the influence of the cavitating geometry. One can easily imagine that a blunt body will cavitate much more intensively than a streamline shaped one.
To show how significant influence the geometry can have we used 4 very similar Venturi shapes and exposed them to the same operating conditions – sequences recorded by the high speed camera (every 6^{th} image is shown – the time difference is 1 ms) at flow rate 105 L/min and cavitation number σ = 1.53 (Eqn. 7) are shown in Fig. 3.

One can see that despite the same convergence angle (18°) cavitation size and appearance varies significantly when the divergence angle is changed. In the case of 4° divergence angle the cavity remains attached – no clouds are shed. On contrary when the angle is increased the clouds are periodically shedding from the attached pocket. The effect is even more pronounced for the case of geometry with sharp transitions (8° S).

Mean cavity length and its dominant pocket shedding frequencies were analyzed and are shown in Fig. 4.

One can see on the diagram on the left that the length of the cavity increases with increasing divergence angle. While the cavitation is practically not visible on a 4° geometry at σ=1.66 its length already exceeds 10mm for the 8 and 12° geometries. The trend continues as the cavitation number is decreased. Similarly significant is the difference between the round and sharp shaped 8° geometries. The difference can be attributed to a larger pressure drop at the transition from the convergent to the divergent part in the sharply shaped Venturi.
The diagram on the right shows the dominant frequencies recorded by the hydrophone. Obviously the pressure pulse frequency is related to the cavitation cloud shedding frequency. It was shown

many times [21] that is related to the size of the cavity and the flow velocity (see also next section), hence it is expected that the 12° geometry will shed clouds less frequently than the 8° or the 8° S geometries. The trend is much different for the case of 4°geometry – this is a result of a different type of cavitation – while we are dealing with developed cavitation in other geometries, the cavitation on a 4° geometry remains attached and no clouds are shed. Intentionally we do not calculate the Strouhal number, which is common in many studies. Here too, one can find many inconsistencies in its definition [21].

Finally the pressure evolutions recorded by the hydrophone for the four investigated geometries are compared in Fig. 5.

One can summarize the pressure evolutions as follows: there are no significant pressure peaks in the 4° geometry – this can clearly be related to the steady and attached nature of cavitation in this Venturi section. The amplitudes increase significantly for the 8° geometry, where unsteady cavitation is present. The pressure oscillates in a similar range in the 12° geometry, but the frequency is somewhat lower, which can be related to the lower cavitation cloud shedding frequency. Finally the most pronounced pressure waves are found in the sharply shaped 8° S geometry, which again correlates well to the unsteady and well defined developed cavitation in this section.

Again one must keep in mind that all recordings are made at the same hydrodynamic conditions. Despite the fact that very similar geometries were compared, significant differences in the topology, dynamics and aggressiveness of cavitation was found.

4.2 Investigation of the influence of flow velocity

The second parameter that should be addressed in all investigations is the influence of the flow velocity. Fig. 6 shows sequences of cavitation in the same geometry (8°), at the same cavitation number (σ=1.53), but at different flow rates.

From the sequences in Fig. 6 no significant differences in cavity appearance can be determined. The only obvious change is the more frequent shedding of the cavitation cloud at higher flow rate (the cloud separated at 7ms for 17.5 m/s, at 6 ms for 20.8 m/s and already at 5 ms for 23.2 m/s). This corresponds to the Strouhal law [21] which states that the shedding frequency should increase with increase of flow velocity and decrease of attached cavity size. Yet, it is also known [22] that the cavity will grow slightly when the flow velocity is increased. These results are presented in more detail in Fig. 7.

Observing the diagram on the left we of course see the increase of cavity length as the cavitation number is decreased. Also, as it was found by Keller [22] we see an increase in the cavity length when the flow velocity is increased at a constant cavitation number. The reason behind this are the increased turbulence level and higher local pressure oscillations which contribute to more fluctuant evaporation [22].
The diagram on the right again proves that both the increase of the velocity and decrease of cavity length contribute to a higher cavitation cloud shedding frequency.

Finally the pressure oscillations are compared for three flow velocities at the same cavitation umber (σ=1.53) in the Venturi 8° geometry.

We see that by the increase of the flow velocity the amplitude of pressure waves generally increases - according to the theory the magnitude of the pressure peaks should increase with the power of 2 (in the case of cavitation erosion, which can many times be used as a measure of the cavitation intensiveness, the increase of damage with flow velocity obeys the power law 6-8 [17]). This can be well seen when one compares the 17.5 m/s, 20.8 m/s and 23.2 m/s cases.

Keeping in mind that we did not vary the cavitation number or the geometry, we again show that the cavitation conditions can be altered only by the change of the flow velocity.

4.3 Investigation of the influence of fluid temperature

At utilization of cavitation a higher temperature of the medium is sometimes required to obtain desirable results [23]. We show three sequences – in all cases the cavitation number (σ=1.53) and the flow velocity (v_{th}=17.5 m/s) is the same, but the temperature varies. The geometry is again the 8° Venturi.

Obviously a significant difference in the size can be seen between the cases at lower temperature and the highest one. Yet in all three cases cavitation remains unsteady and very clear cavitation cloud shedding can be seen.
The trends can be better discussed by observing Fig. 10 where the cavitation length and shedding frequency data is plotted for different water temperatures.

From the diagram on the left we can see that by increasing the medium temperature the cavitation firstly grows, but at an additional increase of the temperature it then shortens to a length much smaller that the initial one. This effect is known as the thermal delay of cavitation [24]. As the temperature is increased the density of the vapor also increases, hence one needs more latent heat to obtain the same mass of vapor. The heat flow from the liquid to the vapor causes the decrease of the liquid temperature and the local drop in evaporation pressure – the formation of the next cavitation bubble is then initiated at a lower pressure and it grows to a smaller size.
The shedding frequencies again prove that the cavitation size is the dominant parameter – the smallest cavity oscillates at the highest frequency.

Fig. 11 shows the pressure evolutions at the same cavitation number (σ=1.53), same velocity (v_{th}=17.5 m/s), in the same geometry (8° Venturi), but at different water temperatures.

The results prove the observations made in studies of cavitation erosion, where many researchers have found that the maximal aggressiveness lies at about 50°C [25]. From Fig. 11 we can see that the magnitude of pressure oscillations increases for temperature of 40°, but then drops significantly for higher temperature case.

One has to acknowledge the undisputed influence and the fact that the cavitation number by itself cannot be a parameter that defines the cavitation conditions.

4.4 Investigation of the influence of fluid quality

Finally we have changed the gas content of the water by degassing it. The sequences at approximately the same cavitation number (σ=1.57), the same flow velocity (v_{th}=19.7 m/s), and geometry (8° Venturi) are shown in Fig. 12.

The size of the cavity remains approximately the same. Also the dynamics – its shedding frequency is not altered significantly by degassing the water, although it seems to be somewhat slower. This was also already shown by Dular et al. [26]. The diagrams in Fig. 13 show the same conclusions.

A significant difference in the length and the shedding frequency cannot be determined. Possibly one can claim that the cavity is larger at high gas content for the cases of high cavitation numbers - generally incipient cavitation number in water with low gas content will be lower [22], but other than that, no difference between the two cases can be claimed.

Much different is the picture when one looks at the pressures (Fig. 14).

Due to smaller amount of micro bubbles and nuclei in the low gas content water the attenuation of the pressure waves, which originate at cavitation cloud collapse, is smaller. Hence the hydrophone recorded much higher pressure oscillations. This again proves that even if the cavitation appears visually the same, its aggressiveness may be different – this fact needs to be considered especially in the cases where different mediums are compared (for example tap water and sea water).

4.5 Investigation of the influence of the cavitation number definition

Previously, we have defined the cavitation number σ by the pressure inside the section upstream of the Venturi (p_c), the velocity at the throat of the Venturi v_{th} (given by the flow rate divided by the throat cross-section) and the vapor pressure and density at the fluid temperature (Eqn. 7).

A reoccurring issue, which contributes significantly to the poor repeatability of the studies is the poor definition of the cavitation number in the manuscripts – the position at which the pressure and the flow velocity were measured or calculated, together with the uncertainty is very rarely given. Moreover researchers tend to use the most convenient value – by this they are not making any error – simply because there is no consent (or standard) which one should be used. Our literature survey revealed the following possible definitions. For pressure:

- pressure inside the reservoir (p_a in the present study),
- pressure in the piping upstream of the cavitation device (p_b in the present study),
- pressure in the cavitation device (upstream of cavitation) (p_c in the present study),
- pressure in the cavitation device (downstream of cavitation) (p_d in the present study),
- pressure in the piping downstream of the cavitation device (p_e in the present study).

Some researchers also consider the pressure inside the cavitation pocket. This is however trivial, since the pressure there should correspond to the vapor pressure – consequently the value of cavitation number should equal 0 (p_v-p_v=0, see Eqn. 5).

The flow velocity can be defined either at the origin of cavitation or at the position of the pressure measurement, hence we have to deal with the following possibilities:

- velocity at the throat of the venturi v_{th},
- velocity in point SP_b - v_b,
- velocity in point SP_c - v_c,
- velocity in point SP_d - v_d,
- velocity in point SP_e - v_e.

Since the free surface inside the reservoir remains at rest, the velocity at point SP_a equals 0. In addition some researchers [27] tend to define the cavitation number by the pressure difference:

$$\sigma = \frac{p_{up} - p_v}{p_{up} - p_{down}}, \tag{8}$$

where p_{up} and p_{down} are pressures upstream and downstream of the cavitating object, respectively.

Finally we end up with 9 possible and legit definitions for the cavitation number: $\sigma_{pa,vth}$, $\sigma_{pb,vth}$, $\sigma_{pb,vb}$, $\sigma_{pc,vth}$, $\sigma_{pc,vc}$, $\sigma_{pd,vth}$, $\sigma_{pd,vd}$, $\sigma_{pe,vth}$, $\sigma_{pe,ve}$, when we use Eqn. 5, and two additional ones: $\sigma_{pb,pe}$, $\sigma_{pc,pd}$, when we use Eqn. 8.

Figure 15 shows the value of the cavitation number for the test case at v_{th} =17.5 m/s and p_c= 243120 Pa at water temperature 21.2°C on a 8° geometry. This time σ was calculated according to all the possible combinations listed above.

The value of cavitation number varies roughly between 1.2 and 168! Please note that the y-axis needed to be broken twice to fit all the values in one diagram. This diagram itself proves that that stating the value of cavitation number as a reference to the operating point is not acceptable.

4.6 Choked flow consideration

We mentioned in the introduction that the usefulness of the cavitation number can become an issue when the flow is choked – when there is a discontinuum of the liquid phase, which occurs when cavitation occupies the whole flow cross-section. From this point on the vapor structure prevents the flow rate from increasing any further. In the present case this occurs at the transition form the developed cavitating flow to supercavitating flow regime. Choked cavitation conditions were first studied by Yan & Thorpe [28] who also suggested the so called choked flow cavitation number (σ_{choked}), which is defined by the flow velocity in the throat v_{th}, the vapour pressure and the pressure downstream of the restriction – p_d in the present study.

$$\sigma_{choked} = \sigma_{pd,vth} = \frac{p_d - p_v}{\frac{\rho v_{th}^2}{2}}. \quad (9)$$

Using this reasoning, we measured the σ_{choked} and obtained values between 0.1 and 0.35. Compared to the regimes, which were studied in during this investigation (for example Fig. 15, $\sigma_{pd,vth} = 1.2$) we see that the choked cavitation numb[illegible]ller – hence the choking was not a issue.

Considering an orifice plate geometry Y[illegible]o derived a theoretical value of the σ_{choked}, which for the present case lies a[illegible]omewhat higher than the measured ones for the Venturi geometries. This is[illegible]ure drop in the Venturi geometry is less pronounced as in the case of flow trans[illegible]e – consequently the flow in the Venturi chokes later.

5 Conclusions

The purpose of the present study is to inform all the researchers and scientists that using solely the cavitation number as a parameter that defines the cavitation conditions is at least insufficient. The lack of data reported in published research is slowing down the progress of methodology. We intentionally used very similar geometries to show the significant difference of cavitation that forms on them.

Figure 16 shows some of the more commonly used geometries by different research groups [4, 12, 23, 29] – hopefully our present paper made it clear how vastly different cavitation will form on such devices, and that the tests cannot be simply compared.

Moreover, in the present study we have only pointed to the most obvious issues (geometry, flow velocity, temperature and gas content) and have omitted more subtle influences such as the size of the device [30] and flow tract surface roughness [31] on the length, dynamics and aggressiveness of cavitating flow.

Finally we have shown that even the definition of cavitation number is an issue. By using commonly accepted values for pressure and flow velocity we could describe the same operating point by cavitation number value that spanned for two orders of magnitude.

To conclude we would like to give the following suggestions for the future reports, which will (we hope) make the research in the filed more transparent and repeatable and will consequently enable faster progress of the science and technology:

1. Effort should be put into an accurate description of the cavitating geometry.
2. If possible images of the cavitation should be provided.
3. If possible pressure fluctuations should be measured.
4. The flow rate should be given.
5. The medium temperature should be given.
6. If possible the gas and solid particle contents of medium should be given.
7. The definition of the cavitation number should be given – with an emphasis how and where the pressure was measured.

References

[1] V. Naddeo, A. Cesaro, D. Mantzavinos, D. Fatta-Kassinos, V. Belgiorno, Water and wastewater disinfection by ultrasound irradiation - a critical review, Global NEST Journal, 16(3), (2014), 561-577.

[2] V.K. Saharan, M.A. Rizwani, A.A. Malani, A.B. Pandit, Effect of geometry of hydrodynamically cavitating device on degradation of Orange-G, Ultrason. Sonochem., 20 (2013), 345–353.

[3] S. Raut-Jadhav, V. Kumar, S. D. Pinjari, S. Sonawane, D. Saini, A. Pandit, Synergetic effect of combination of AOP's (hydrodynamic cavitation and H2O2) on the degradation of neonicotinoid class of insecticide, Journal of Hazardous Materials, 261, (2013), 139–147.

[4] M. Sivakumar, A.B. Pandit, Water treatment: a novel energy efficient hydrodynamic cavitational technique, Ultrason. Sonochem., 9 (2002), 123–131.

[5] M.P. Badve, T. Alpar, A.B. Pandit, P.R. Gogate, L. Csoka, Modeling the shear rate and pressure drop in a hydrodynamic cavitation reactor with experimental validation based on KI decomposition studies, Ultrasonics Sonochemistry, 22, (2015), 272-277.

[6] M.V. Bagal, P.R. Gogate, Wastewater treatment using hybrid treatment schemes based on cavitation and Fenton chemistry: A review, Ultrasonics Sonochemistry, 21, (2014), 1–14.

[7] P.R Gogate, Cavitation: an auxiliary technique in wastewater treatment schemes, Advances in Environmental Research, 6(3), (2002), 335-358.

[8] M. Capocelli, M. Prisciandaro, A. Lancia, D. Musmarra, Hydrodynamic cavitation of p-nitrophenol: A theoretical and experimental insight, Chemical Engineering Journal, 254, (2014), 1-8.

[9] X. Wang, Y. Zhang, Degradation of alachlor in aqueous solution by using hydrodynamic cavitation, Journal of Hazardous Materials, 161(1), (2009), 202-207.

[10] M.M. Gore, V. K. Saharan, D.V. Pinjari, P.V. Chavan, A.B. Pandit, Degradation of reactive orange 4 dye using hydrodynamic cavitation based hybrid techniques, Ultrasonics Sonochemistry, 21(3), (2014), 1075-1082.

[11] P.S. Kumar, M.S. Kumar, A.B Pandit, Experimental quantification of chemical effects of hydrodynamic cavitation, Chemical Engineering Science, 55(9), (2000), 1633-1639.

[12] S.S. Sawant, A. C. Anil, V. Krishnamurthy, C. Gaonkar, J. Kolwalkar, L. Khandeparker, D. Desai, A. V. Mahulkar, V. V. Ranade, A. B. Pandit, Effect of hydrodynamic cavitation on zooplankton: A tool for disinfection, Biochemical Engineering Journal, 42(3), (2008), 320-328.

[13] Z. Wu, H. Shen, B. Ondruschka, Y.Zhang, W. Wang, D. H. Bremner, Removal of blue-green algae using the hybrid method of hydrodynamic cavitation and ozonation, Journal of Hazardous Materials, 235–236, (2012), 152–158.

[14] J.G.D. Filho, M.P. Assis, A.I. Borri Genovez, Bacterial inactivation in artificially and naturally contaminated water using a cavitating jet apparatus, Journal of Hydro-environment Research, 9(2), (2015), 259–267.

[15] S. Arrojo, Y. Benito A. Martínez Tarifa, A parametrical study of disinfection with hydrodynamic cavitation, Ultrasonics Sonochemistry, 15(5), (2008), 903–908.

[16] L. Mezule, S. Tsyfansky, V. Yakushevich, T. Juhna, A simple technique for water disinfection with hydrodynamic cavitation: Effect on survival of Escherichia coli, Desalination 248 (2009) 152–159.

[17] M. Dular, B. Sirok, B. Stoffel, Influence of gas content in water and flow velocity on cavitation erosion aggressiveness, Journal of Mechanical Engineering 51 (2005) 132–145.

[18] F. Brand, Ein physikalisches Verfahren zur Bestimmung von geloesten und ungeloesten Gasen in Wasser, Voith Forschung und Konstruktion 27 (1981).

[19] F.B. Peterson, Hydrodynamic cavitation and some considerations of the influence of free gas content, in: Proceedings of the 9th Symposium on Naval Hydrodynamics, (1972).

[20] R.E.A. Arndt, A.P. Keller, Free gas content effects on cavitation inception and noise in a free shear flow, in: Proceedings of the IAHR Symposium Two Phase Flow and Cavitation in Power Generation Systems, Grenoble, (1976).

[21] M. Dular, R. Bachert, The Issue of Strouhal Number Definition in Cavitating Flow, Journal of Mechanical Engineering 55(11), (2009), 666-674.

[22] A.P. Keller, Cavitation Scale Effects - Empirically Found Relations and the Correlation of Cavitation Number and Hydrodynamic Coefficients. Fourth International Symposium on Cavitation, (2001).

[23] M. Zupanc, T. Kosjek, M. Petkovšek, M. Dular, B. Kompare, B. Širok, Ž. Blažeka, E. Heath, Removal of pharmaceuticals from wastewater by biological processes, hydrodynamic cavitation and UV treatment. Ultrasonics Sonochemistry, 20(4), (2013), 1104-1112.

[24] M. Petkovšek, M. Dular IR measurements of the thermodynamic effects in cavitating flow, International Journal of Heat and Fluid Flow, 44, (2013), 756-763.

[25] M. Dular, Hydrodynamic cavitation damage in water at elevated temperatures, Wear, 346–347, (2016), 78-86.

[26] M. Dular, B. Bachert, B. Stoffel, B. Širok, Relationship between cavitation structures and cavitation damage, Wear, 257(11), (2004), 1176-1184.

[27] B.V. Hubballi, V.B. Sondur, A Review on the Prediction of Cavitation Erosion Inception in Hydraulic Control Valves, International Journal of Emerging Technology and Advanced Engineering, 3(1), (2013), 110-119.

[28] Y. Yan, R.B. Thorpe, Flow regime transitions due to cavitation in the flow through an orifice, Int. J. Multiphase Flow, Vol. 16(6), (1990), 1023-1045.

[29] M. Petkovšek, M. Zupanc, M. Dular, T. Kosjek, E. Heath, B. Kompare, B. Širok, Rotation Generator of Hydrodynamic Cavitation for Water Treatment, Separation and Purification Technology, 118, (2013), 415–423.

[30] M. Dular, I. Khlifa, S. Fuzier, A.M. Mahamadou, O. Coutier-Delgosha, Scale effect on unsteady cloud cavitation. Exp. fluids, 53(5), (2012), 1233-1250.

[31] O. Coutier-Delgosha, J. Devillers, M. Leriche, T. Pichon, Effect of wall roughness on the dynamics of unsteady cavitation, J. Fluids Eng., 127(4), (2005), 726–733.

Figure captions

Figure 1: Cavitation test-rig.

Fig. 2 The specifications of four Venturi-type sections (18°/4°, 18°/8°, 18°/12° and 18°/8° S) and the positions of static ($SP_{b, c, d, e}$) and dynamic (DP) pressure acquisition.

Figure 3: Sequences of cavitation evolution at the same cavitation number (σ=1.53), same velocity (v_{th}=17.5 m/s) but in different geometries.

Figure 4: Mean cavity length (left) and shedding frequencies (right) for the same velocity (v_{th}=17.5 m/s) but in different geometries.

Figure 5: Pressure oscillations for the same cavitation number, same velocity but in different geometries.

Figure 6: Sequences of cavitation evolution at the same cavitation number (σ=1.53), but different velocities.

Figure 7: Mean cavity length (left) and shedding frequencies (right) as a function of flow velocity.

Figure 8: Pressure oscillations for the same cavitation number (σ=1.53) but different velocities.

Figure 9: Sequences of cavitation evolution at the same cavitation number (σ=1.53) and the flow velocity (v_{th}=17.5 m/s) but at different temperatures.

Figure 10: Mean cavity length (left) and shedding frequencies (right) as a function of temperature.

Figure 11: Pressure oscillations for the same cavitation number (σ=1.53), same velocity (v_{th}=17.5 m/s), but at different temperatures.

Figure 12: Sequences of cavitation evolution at the same cavitation number (σ=1.57), same velocity (v_{th}=19.7 m/s) but different water gas content.

Figure 13: Mean cavity length (left) and shedding frequencies (right) as a function of gas content.

Figure 14: Pressure oscillations for the same cavitation number (σ=1.57), same velocity (v_{th}=19.7 m/s) but different water gas contents.

Figure 15: The value of cavitation number s for test case 1, calculated according to different definitions of pressure and velocity.

Figure 16: The wide variety of geometries used in the studies of utilization of hydrodynamic cavitation. Adopted from [4, 12, 23, 29].

Figure01

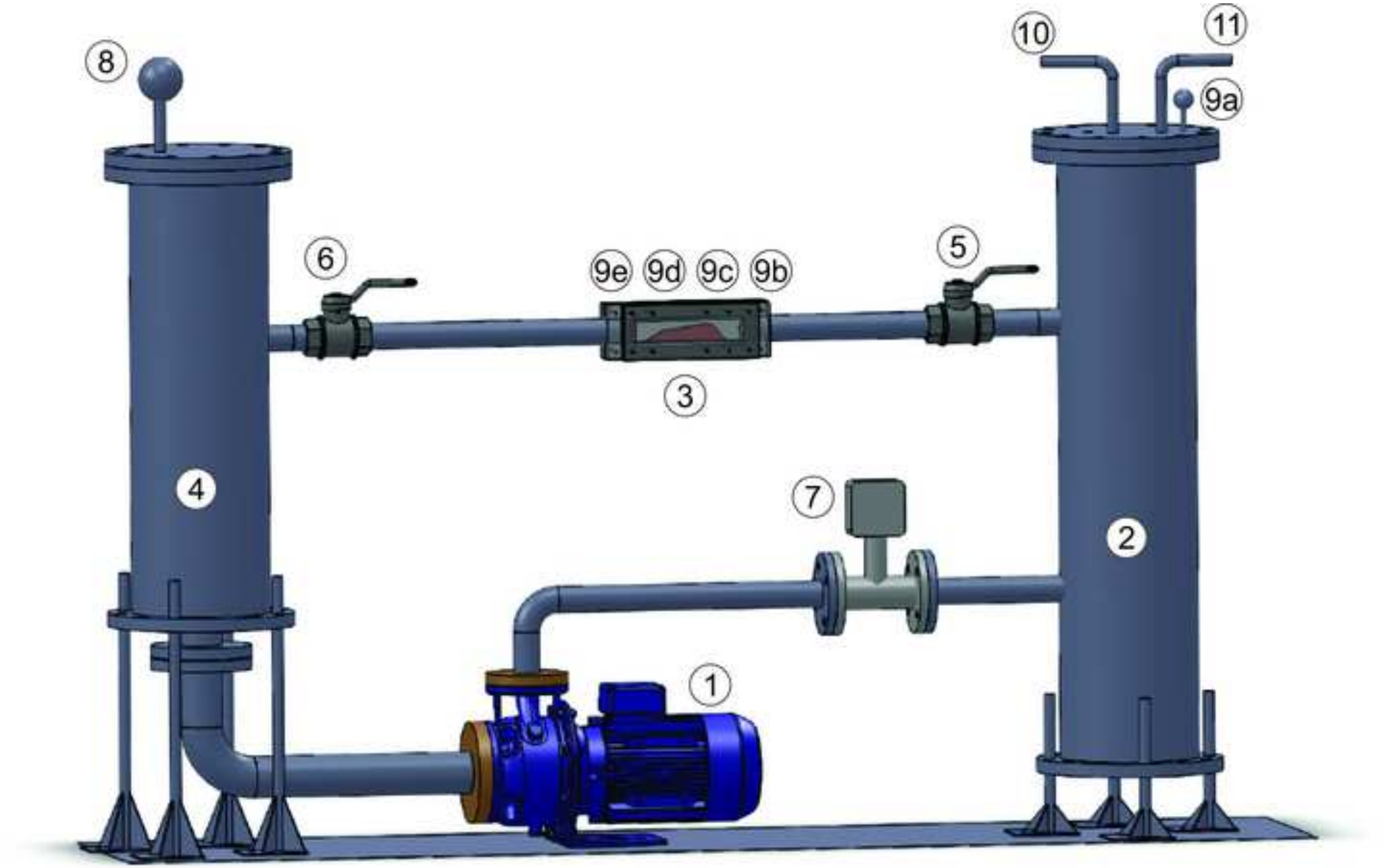

Figure02

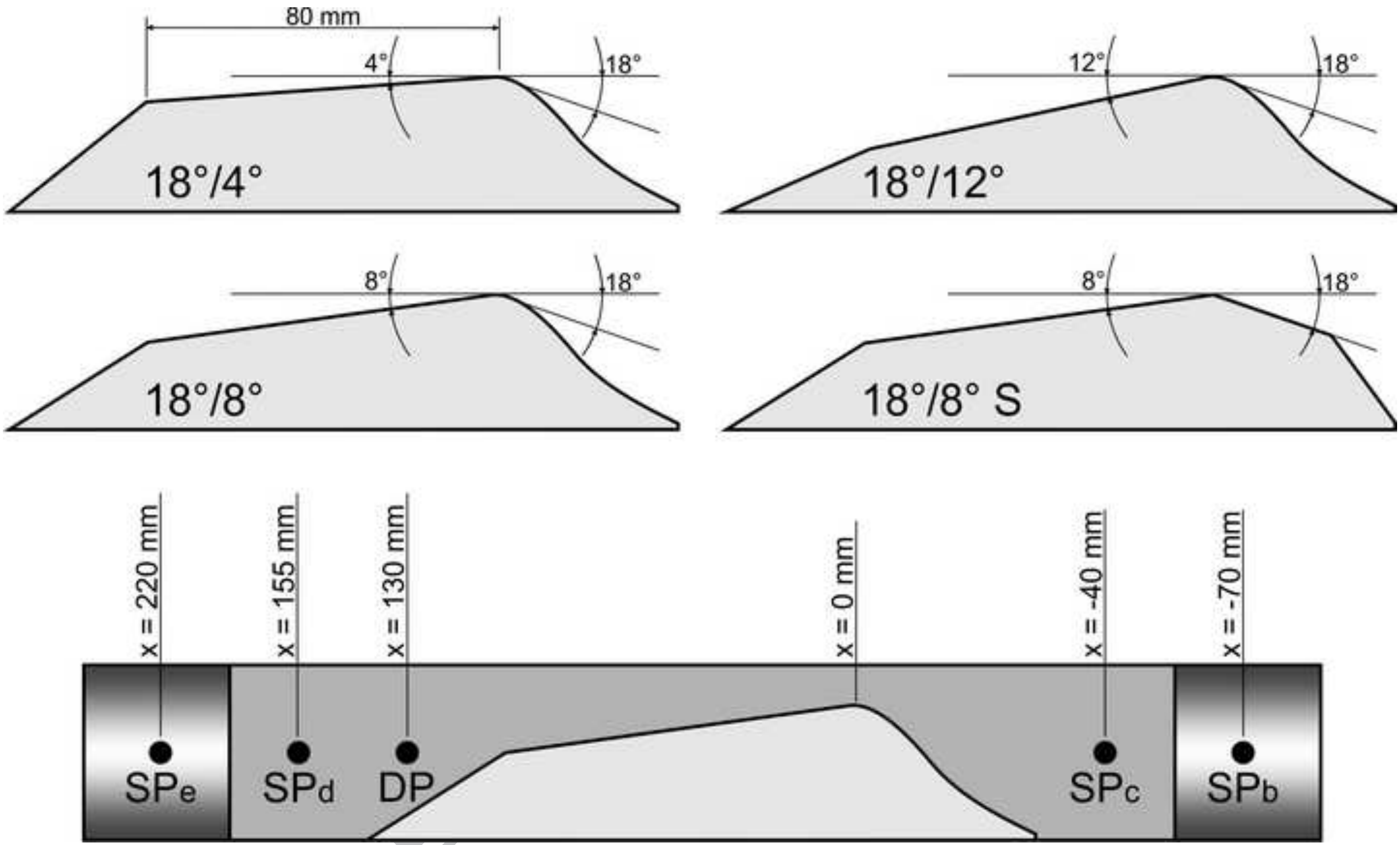
80 mm
4°
18°
18°/4°
12°
18°
18°/12°
8°
18°
18°/8°
8°
18°
18°/8° S
x = 220 mm
x = 155 mm
x = 130 mm
x = 0 mm
x = -40 mm
x = -70 mm
SPe
SPd
DP
SPc
SPb

Figure03

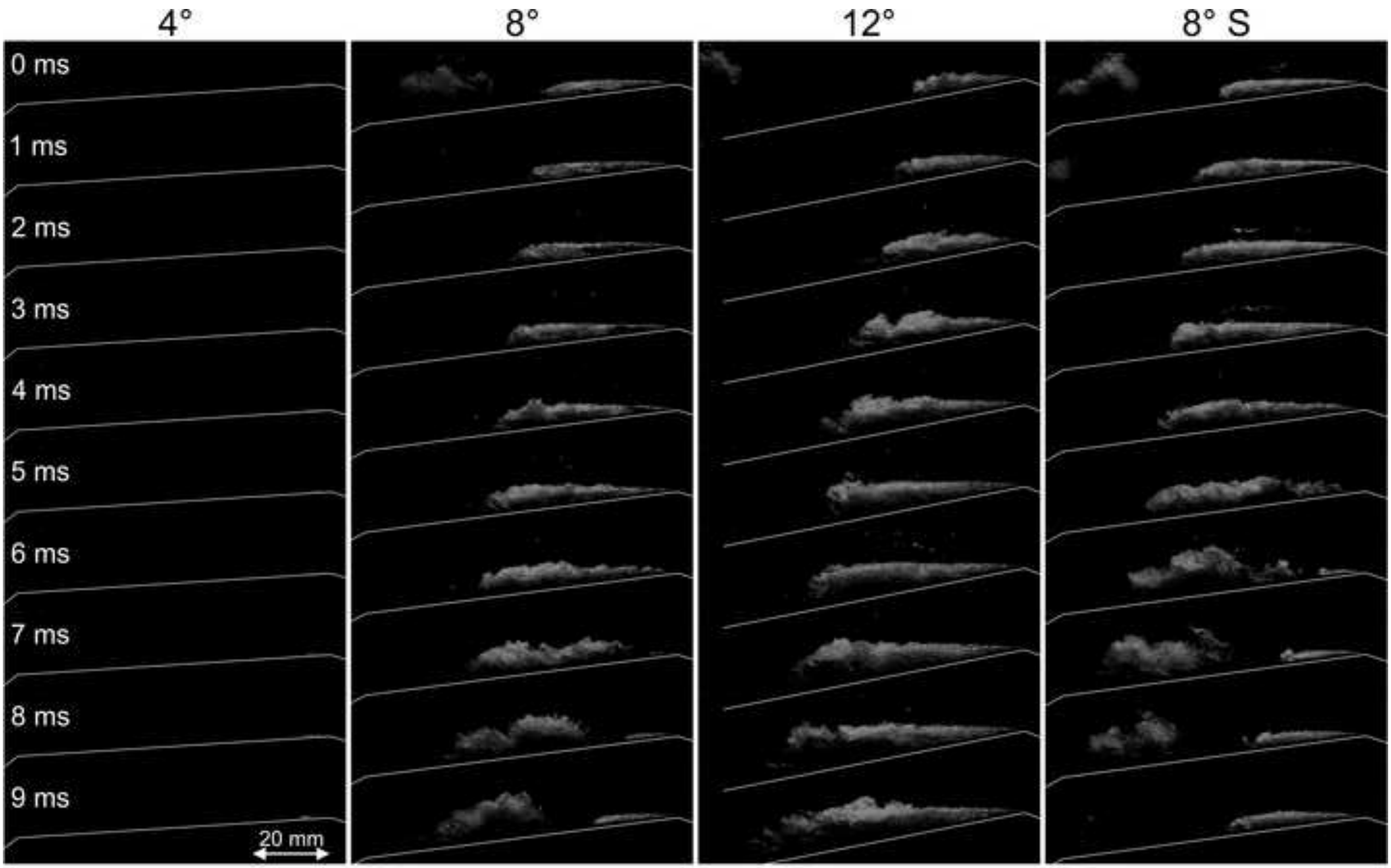

Figure04

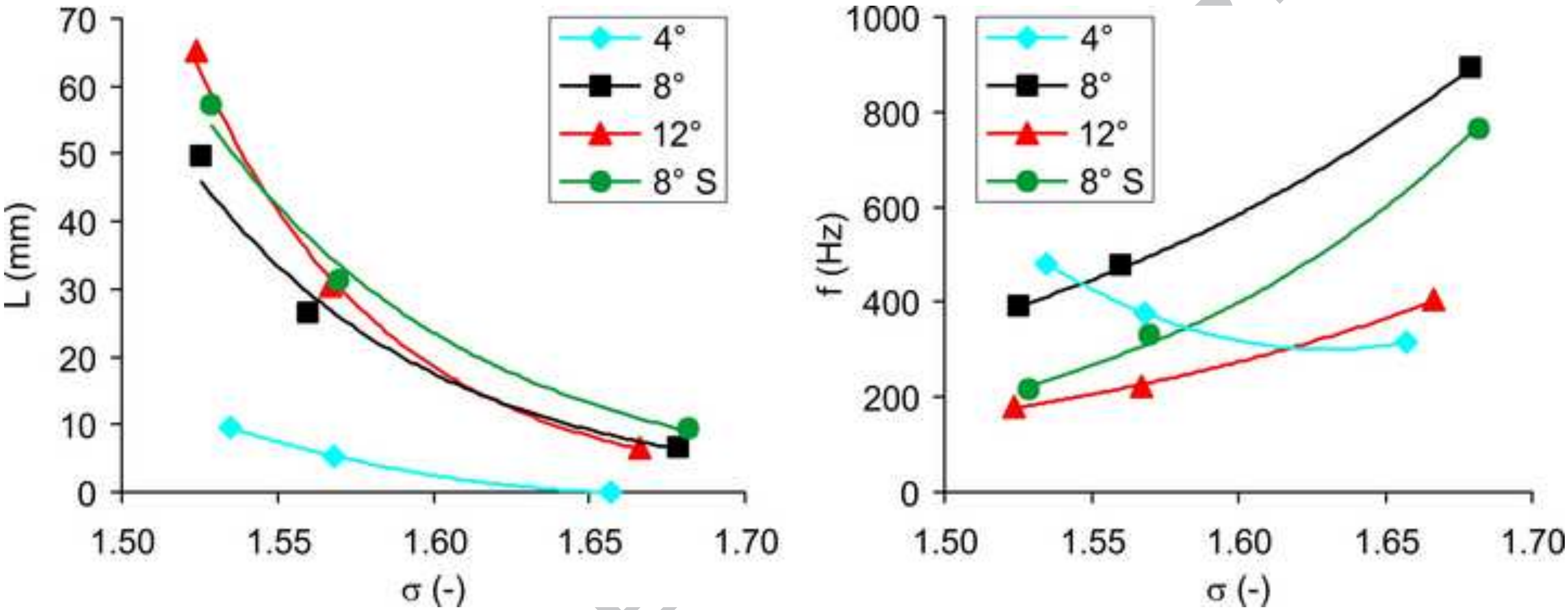

L (mm)
70
60
50
40
30
20
10
0
1.50
1.55
1.60
1.65
1.70
σ (-)
4°
8°
12°
8° S
f (Hz)
1000
800
600
400
200
0
1.50
1.55
1.60
1.65
1.70
σ (-)
4°
8°
12°
8° S

Figure05

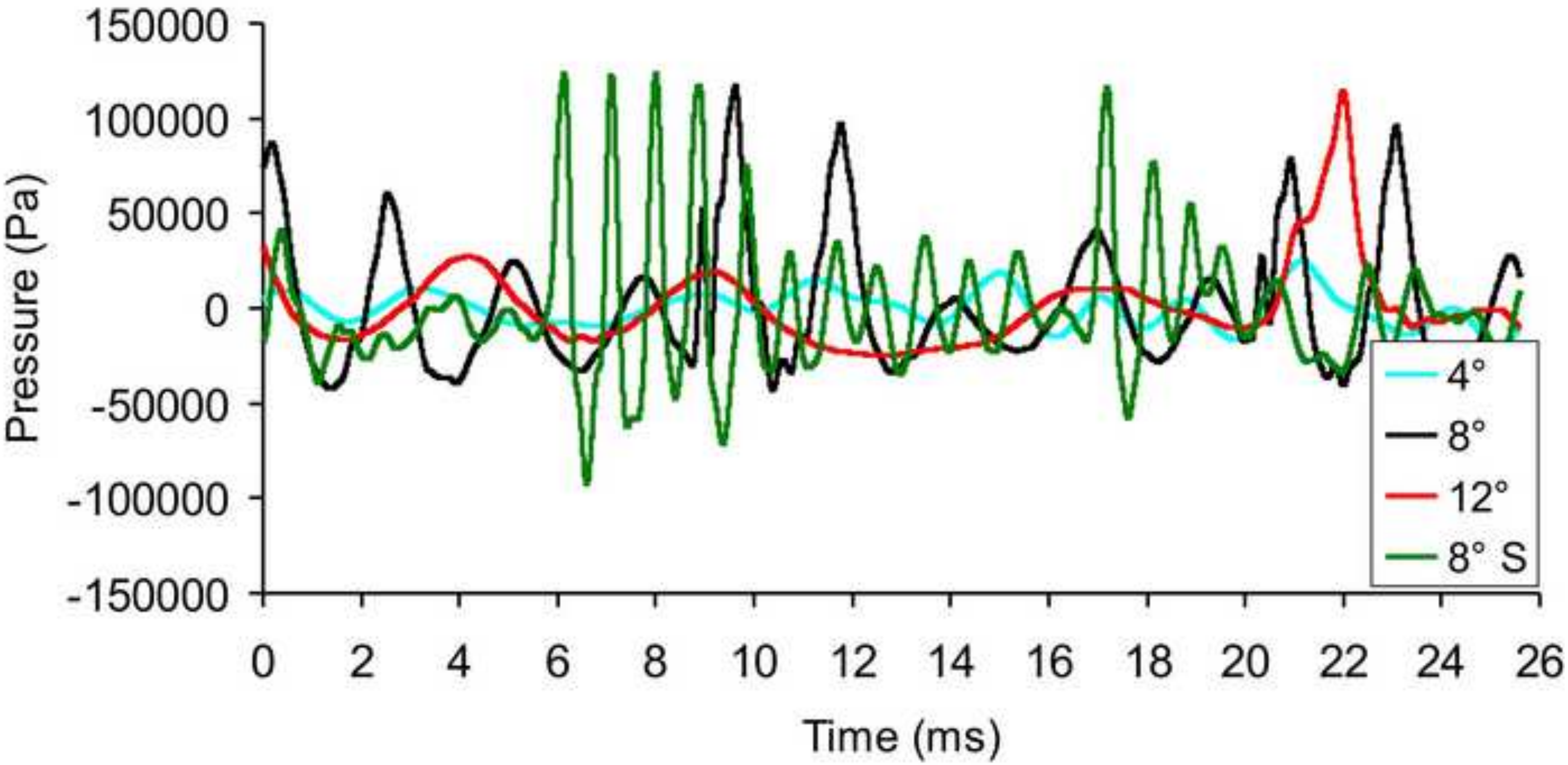

150000
100000
50000
0
-50000
-100000
-150000
Pressure (Pa)
0
2
4
6
8
10
12
14
16
18
20
22
24
26
Time (ms)
4°
8°
12°
8° S

Figure06

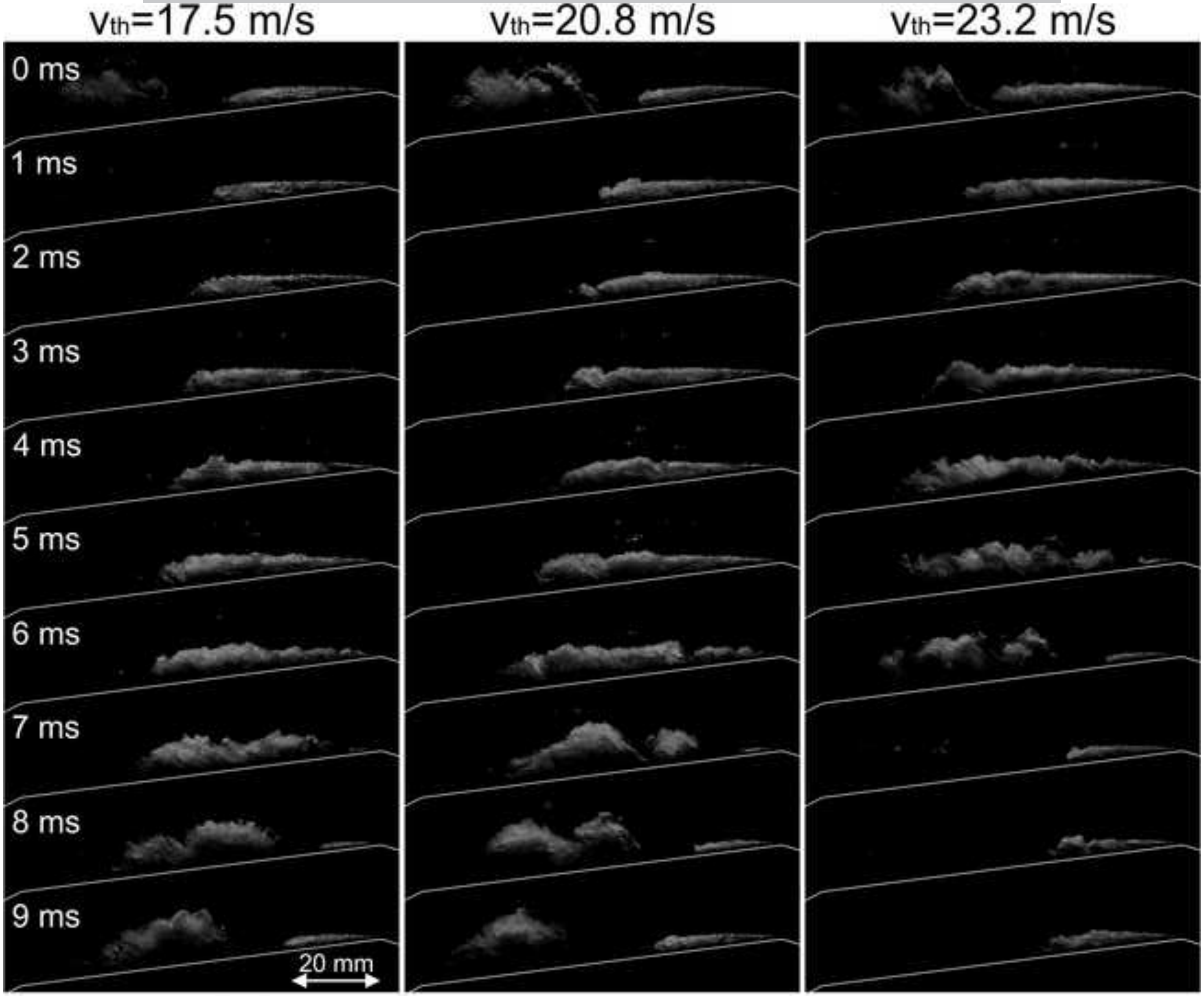

v_{th}=17.5 m/s
v_{th}=20.8 m/s
v_{th}=23.2 m/s
0 ms
1 ms
2 ms
3 ms
4 ms
5 ms
6 ms
7 ms
8 ms
9 ms
20 mm

Figure07

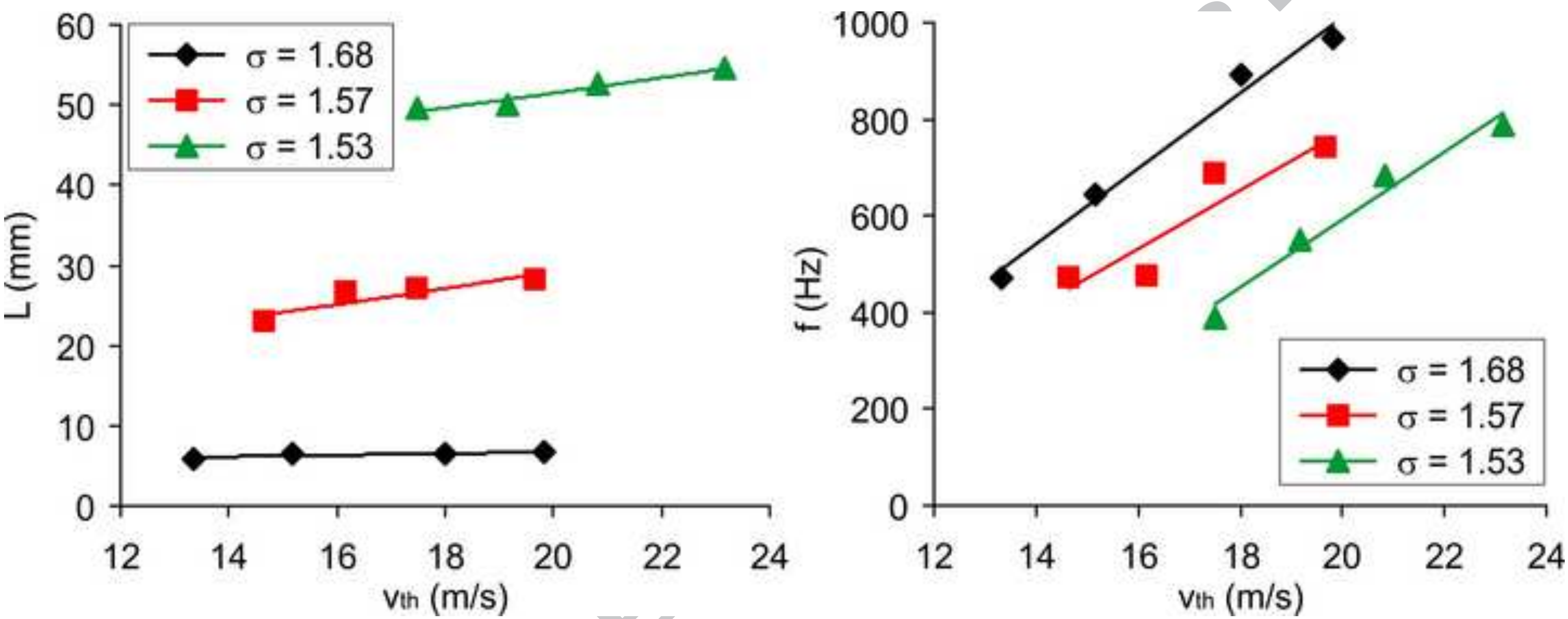

60
50
40
30
20
10
0
L (mm)
12
14
16
18
20
22
24
vth (m/s)
σ = 1.68
σ = 1.57
σ = 1.53
1000
800
600
400
200
0
f (Hz)
12
14
16
18
20
22
24
vth (m/s)
σ = 1.68
σ = 1.57
σ = 1.53

Figure08

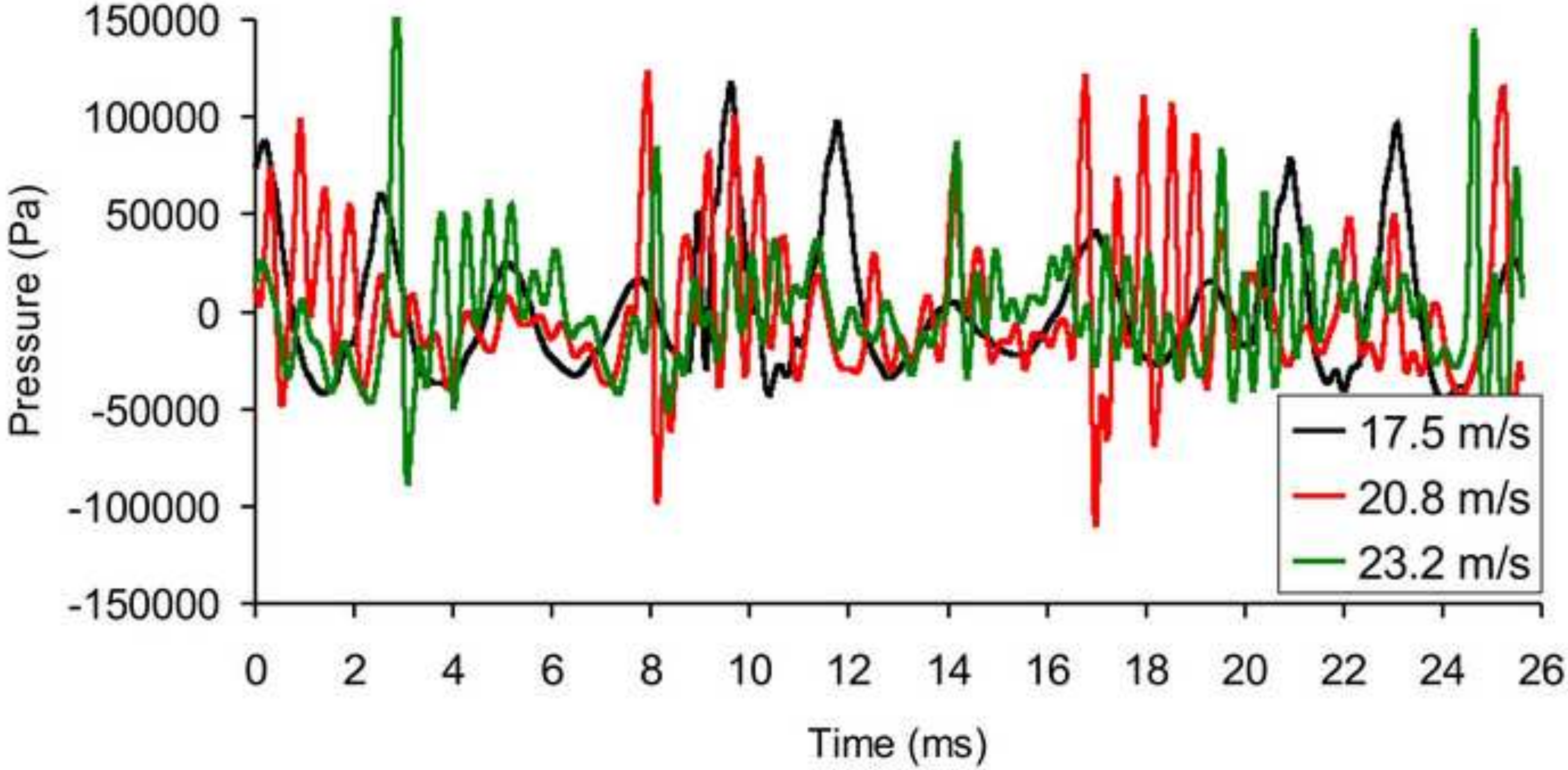
150000
100000
50000
0
-50000
-100000
-150000
Pressure (Pa)
0
2
4
6
8
10
12
14
16
18
20
22
24
26
Time (ms)
17.5 m/s
20.8 m/s
23.2 m/s

Figure09

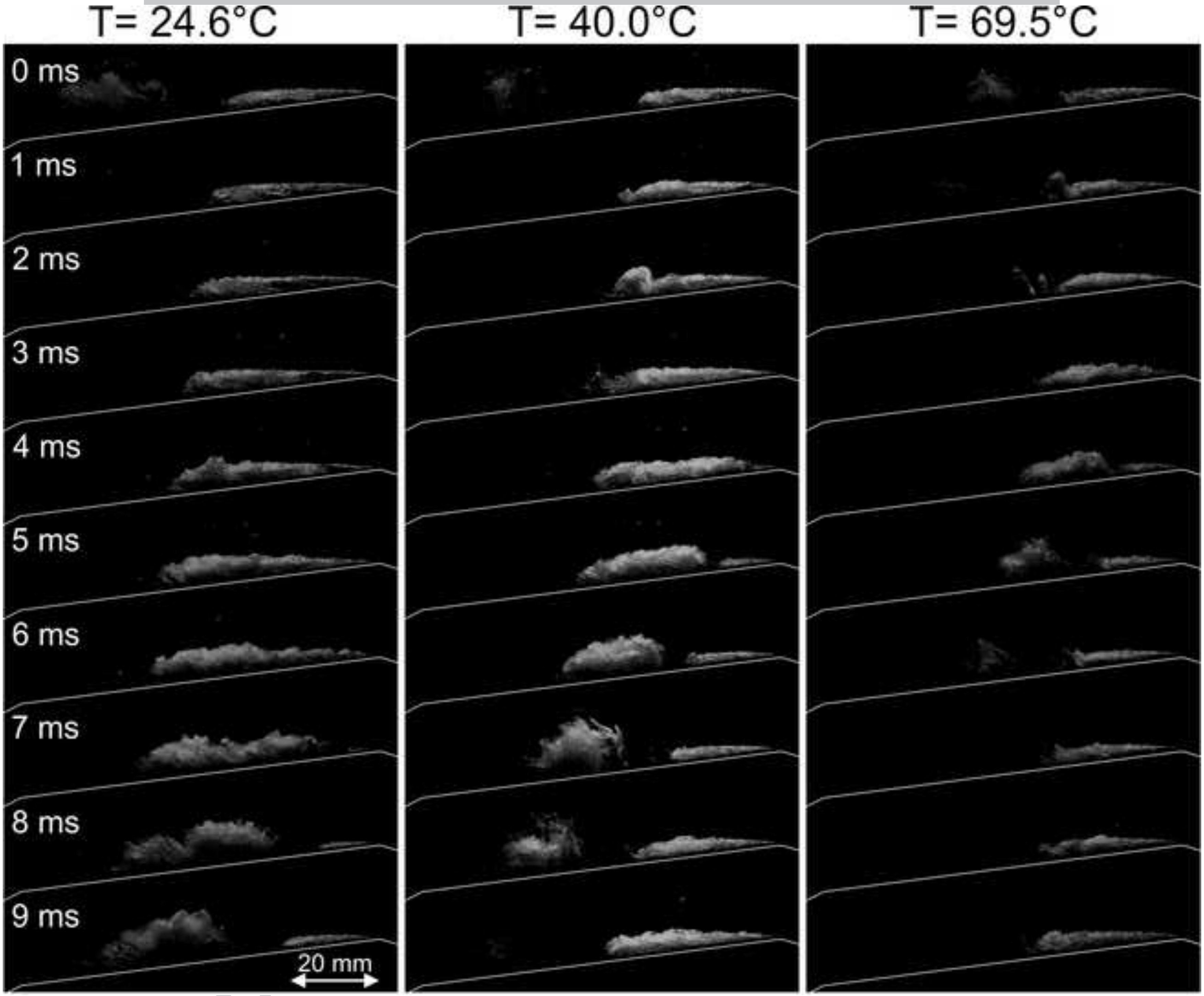

Figure10

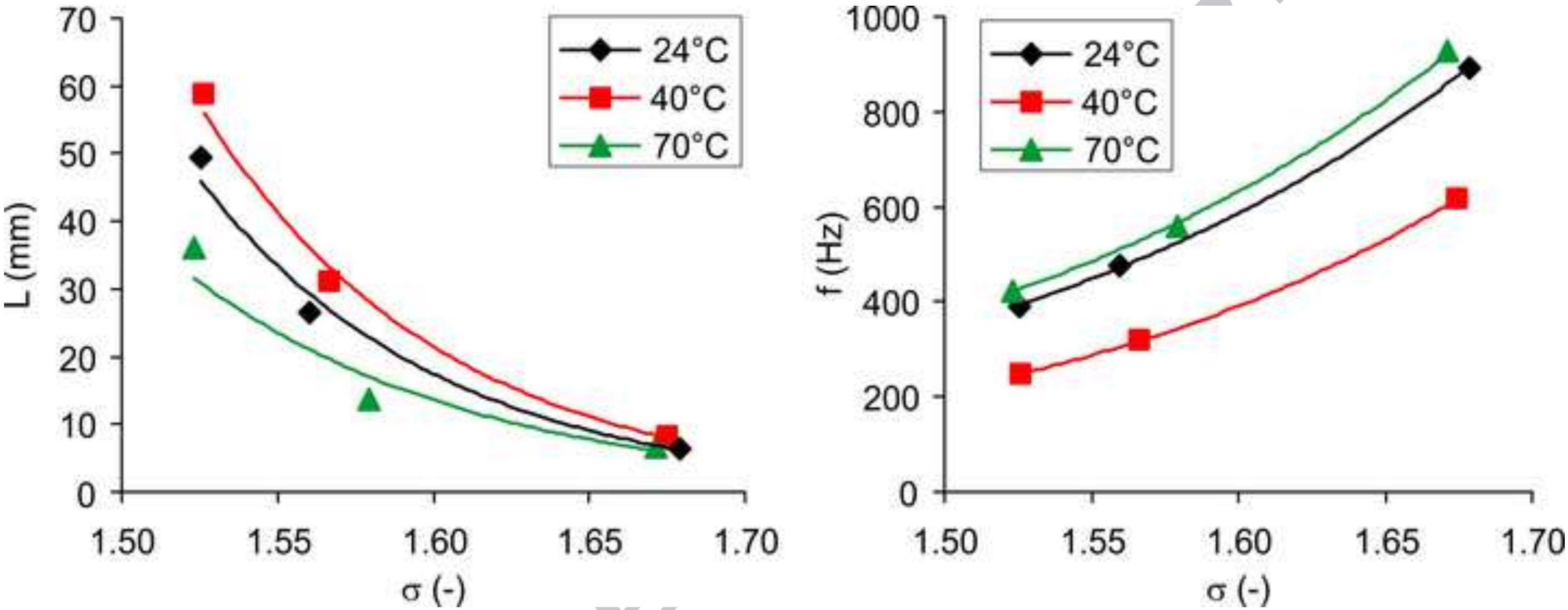
70
60
50
40
30
20
10
0
L (mm)
1.50
1.55
1.60
1.65
1.70
σ (-)
24°C
40°C
70°C
1000
800
600
400
200
0
f (Hz)
1.50
1.55
1.60
1.65
1.70
σ (-)
24°C
40°C
70°C

Figure11

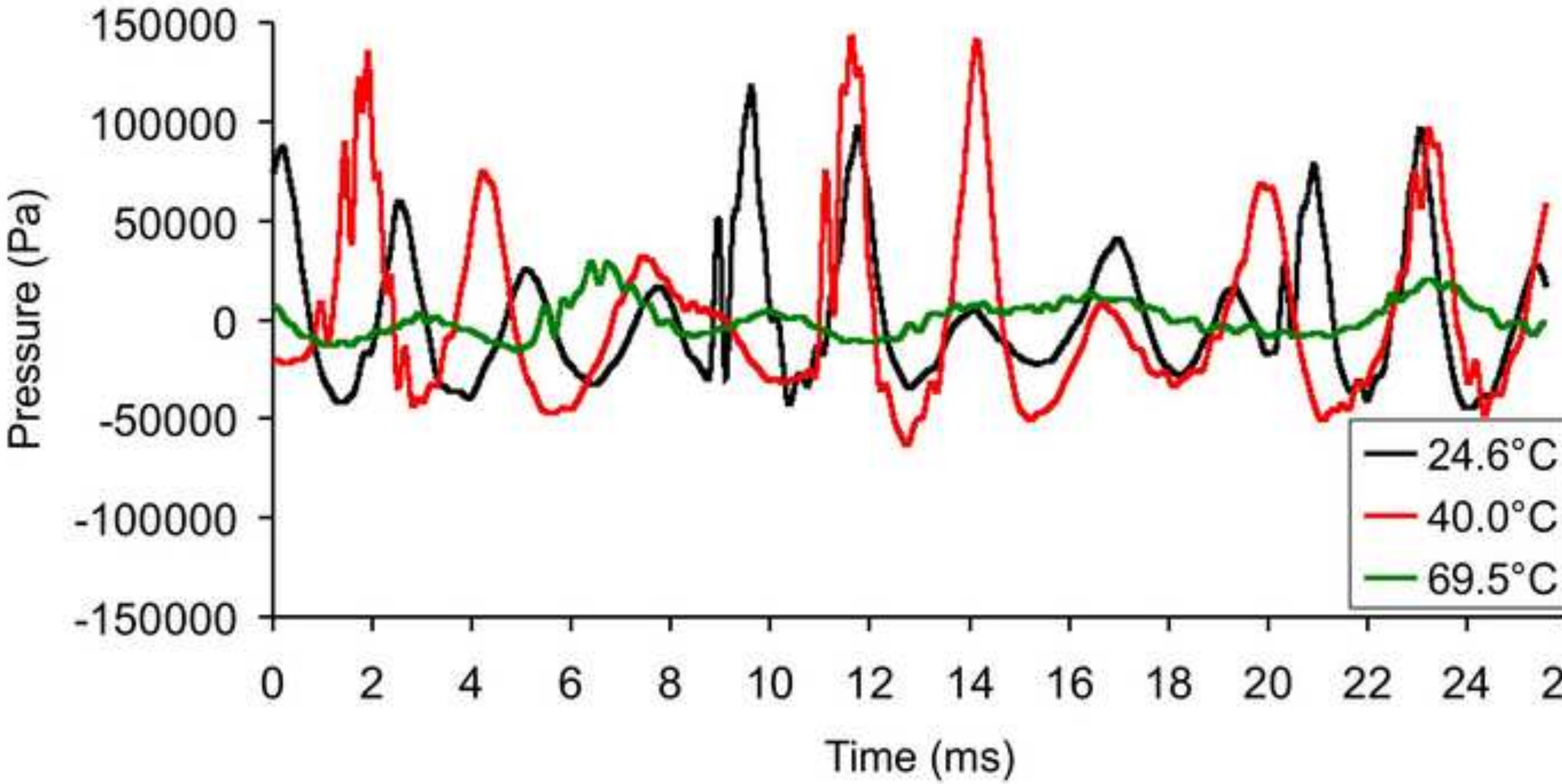

150000
100000
50000
0
-50000
-100000
-150000
Pressure (Pa)
0
2
4
6
8
10
12
14
16
18
20
22
24
26
Time (ms)
24.6°C
40.0°C
69.5°C

Figure12

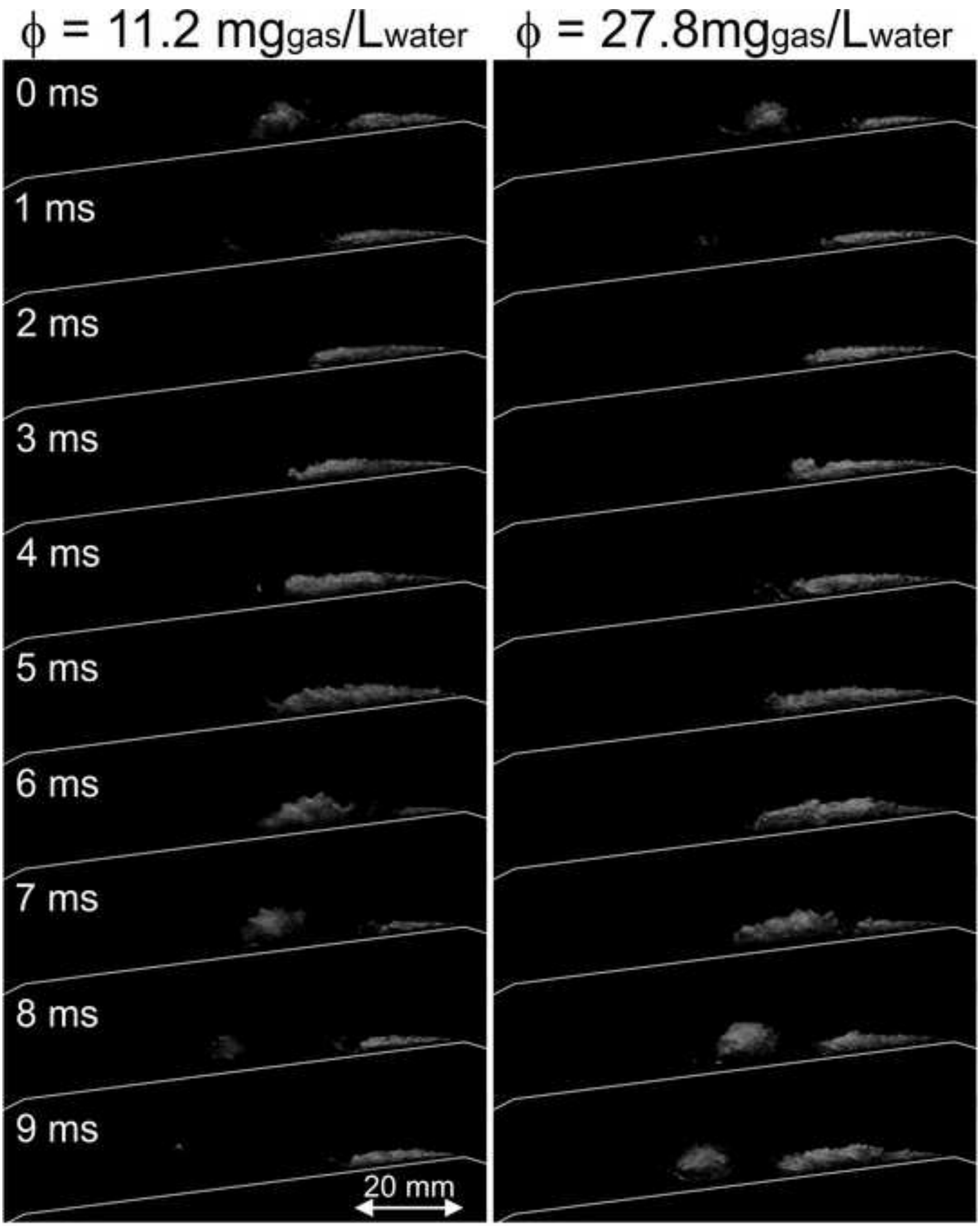
ϕ = 11.2 mggas/Lwater
ϕ = 27.8mggas/Lwater
0 ms
1 ms
2 ms
3 ms
4 ms
5 ms
6 ms
7 ms
8 ms
9 ms
20 mm

Figure13

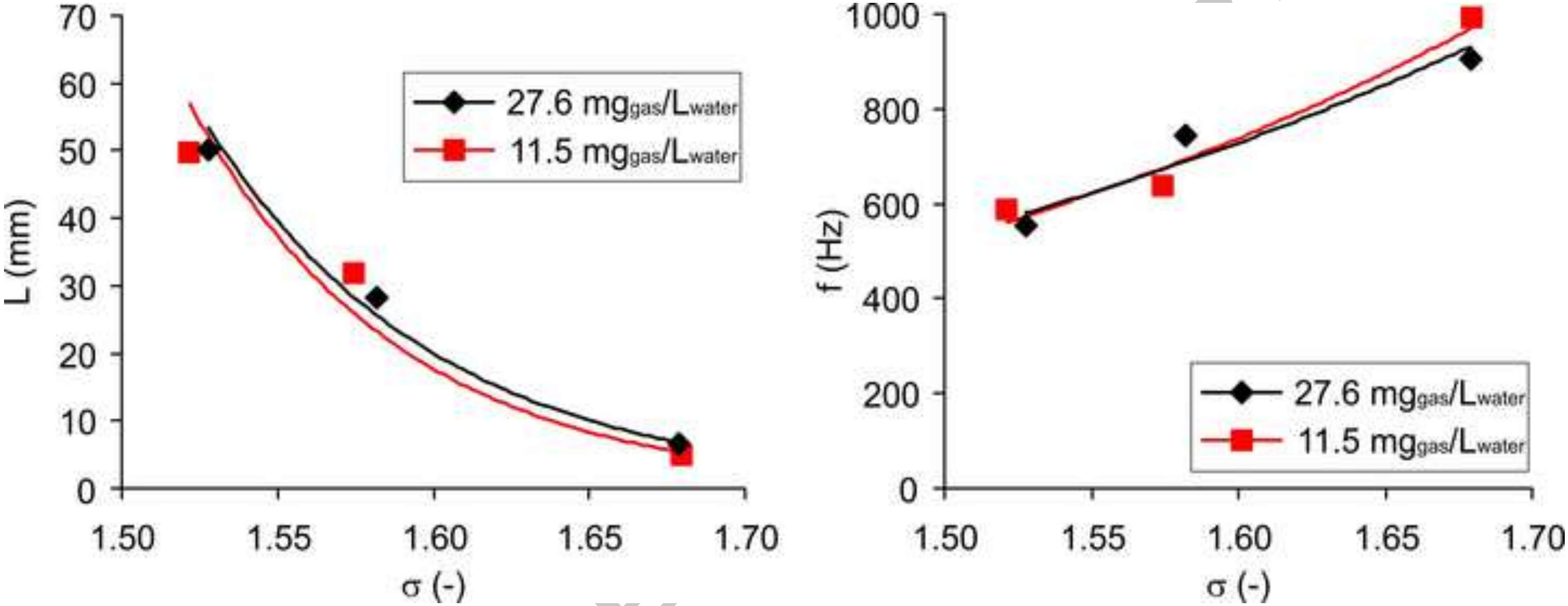

70
60
50
40
30
20
10
0
L (mm)
27.6 mggas/Lwater
11.5 mggas/Lwater
1.50
1.55
1.60
1.65
1.70
σ (-)
1000
800
600
400
200
0
f (Hz)
27.6 mggas/Lwater
11.5 mggas/Lwater
1.50
1.55
1.60
1.65
1.70
σ (-)

Figure14

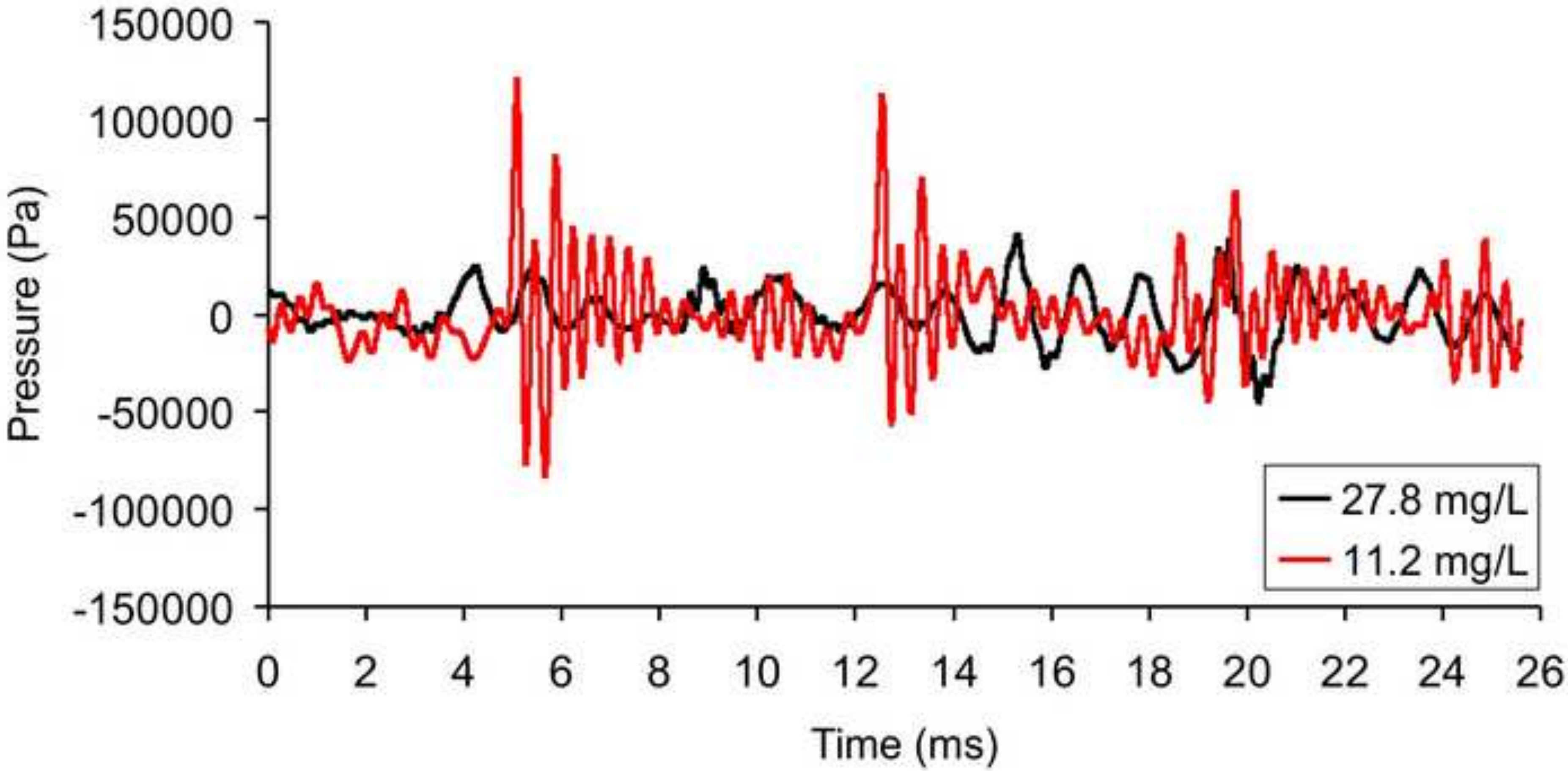
150000
100000
50000
0
-50000
-100000
-150000
Pressure (Pa)
0
2
4
6
8
10
12
14
16
18
20
22
24
26
Time (ms)
27.8 mg/L
11.2 mg/L

Figure15

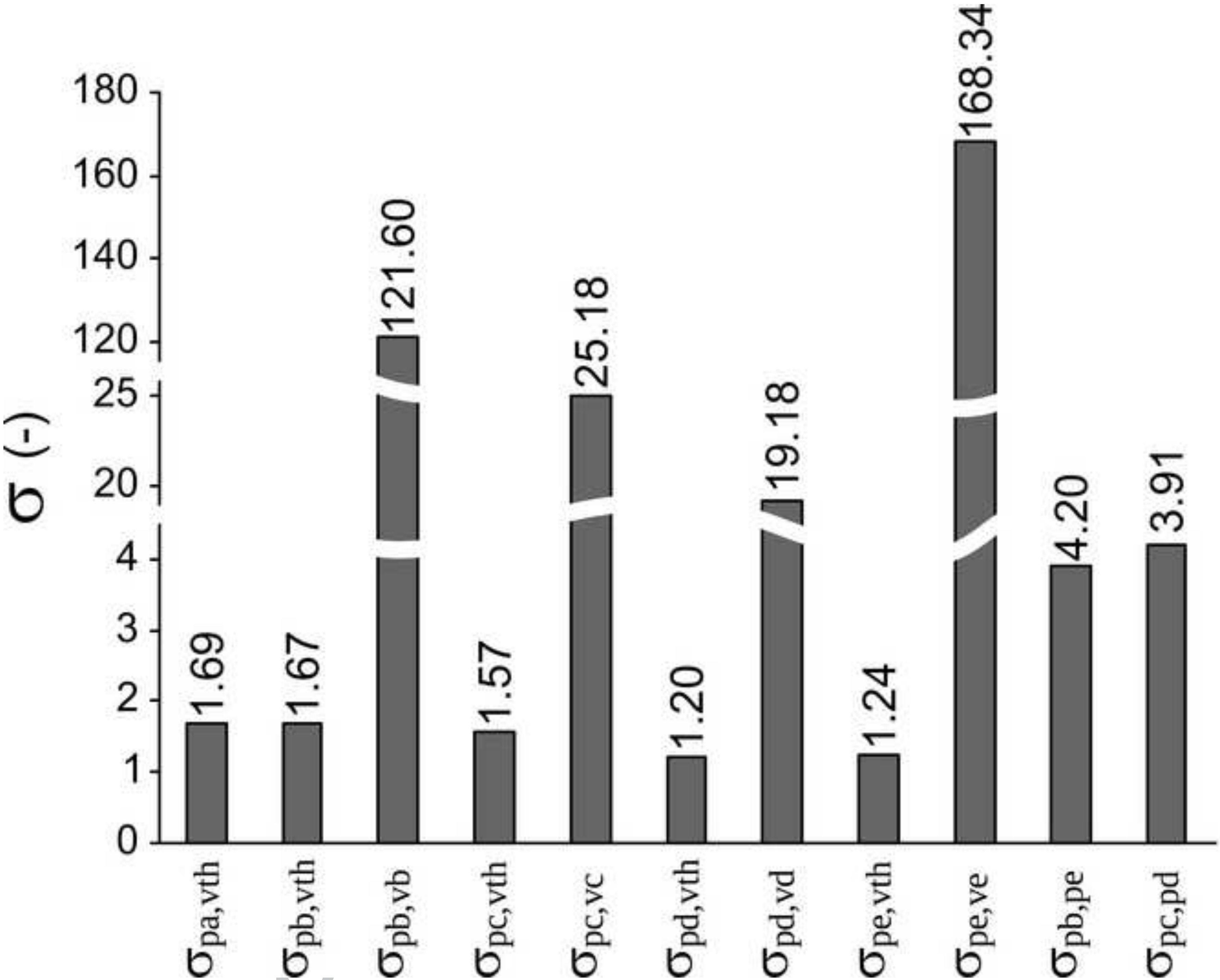
σ (-)
180
160
140
120
25
20
4
3
2
1
0
1.69
1.67
121.60
1.57
25.18
1.20
19.18
1.24
168.34
4.20
3.91
σpa,vth
σpb,vth
σpb,vb
σpc,vth
σpc,vc
σpd,vth
σpd,vd
σpe,vth
σpe,ve
σpb,pe
σpc,pd

Figure16

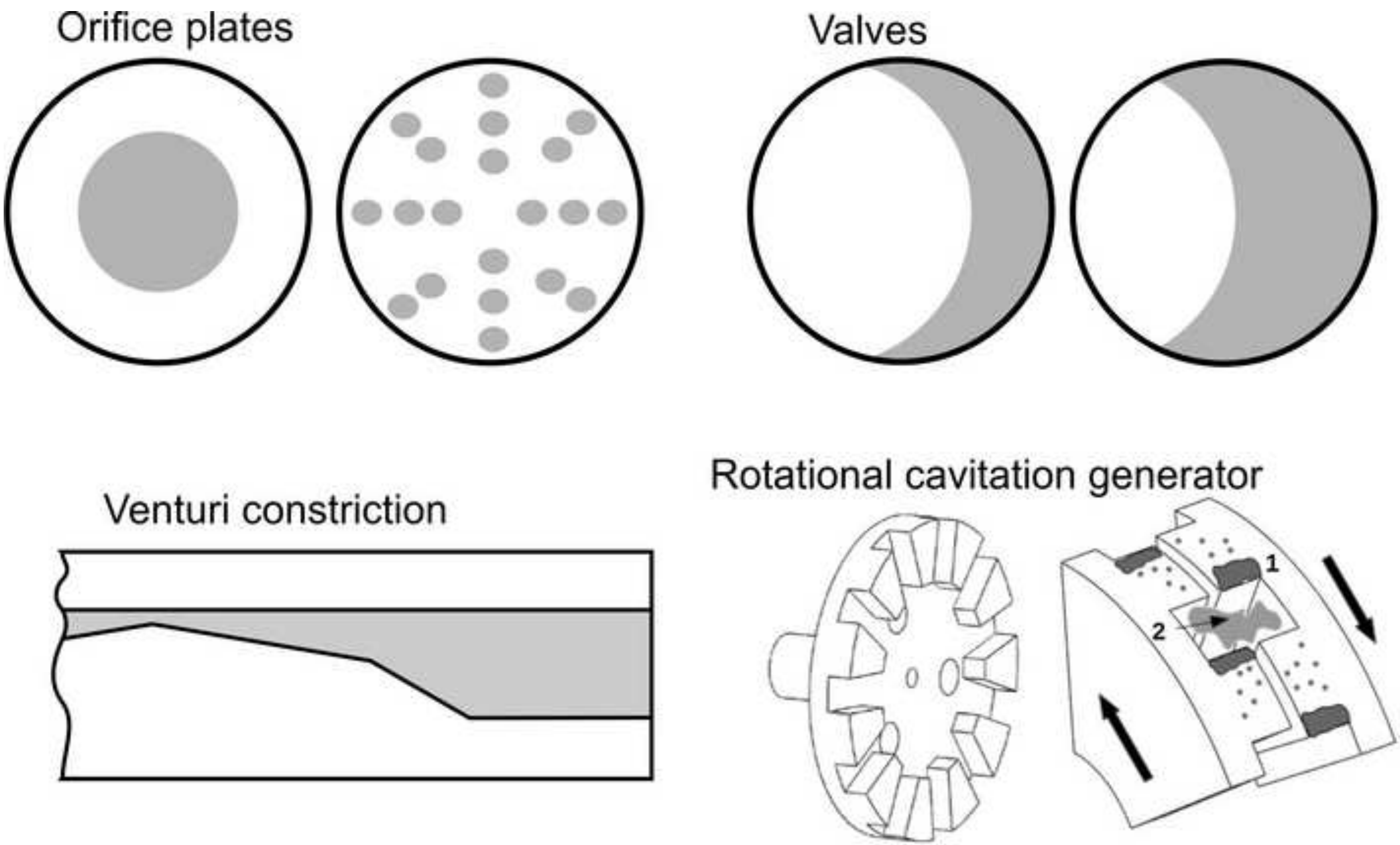
Orifice plates
Valves
Venturi constriction
Rotational cavitation generator
1
2

Highlights

- Big inconsistencies in studies of utilization of cavitation exist
- Studies are many times not repeatable
- Cavitation conditions cannot be described by the σ value
- Results show obvious issues of using σ value
- Effort should be put into description of methods